3-Deazaneplanocin A and Neplanocin A analogs and their effects on apoptotic cell death

Eric K. W. Tam,[a] Tuan Minh Nguyen,[a] Cheryl Z.H. Lim,[b] Puay Leng Lee,[b] Zhimei Li,[b] Xia Jiang,[b] Sridhar Santhanakrishnan,[a] Tiong Wei Tan,[a] Yi Ling Goh,[a] Sze Yue Wong,[a] Haiyan Yang,[a] Esther H.Q. Ong,[c] Jeffrey Hill,[c] Qiang Yu,*[b] and Christina L. L. Chai*[a, d]

Abstract: 3-Deazaneplanocin A (DzNep) is a potential epigenetic drug for the treatment of various cancers. DzNep has been reported to deplete cellular EZH2 complex, giving rise to epigenetic modifications which reactivates many silenced tumour suppressors in cancer cells. Despite its promise as an anti-cancer drug, the mechanism of EZH2 depletion is not understood. In this study, a number of analogs of DzNep were examined for DzNep-like activities in their ability to induce synergistic apoptosis in cancer cells in combination with Trichostatin A. The structure-cell activity relationships thus obtained provided valuable information on the structural requirements for biological activities. The studies identified three compounds that show similar activities to DzNep. Two of these compounds show good pharmacokinetics and safety profile. Western blot studies with selected DzNep analogs verify that the compounds behave analogously to DzNep in their ability to deplete histone methylation. Attempts to correlate the observed synergistic apoptotic activities with measured *S*-Adenosylhomocysteine hydrolase inhibitory (SAHH) activities suggest that the apoptotic activity may not be directly due to its SAHH activity.

Introduction

Epigenetic alterations play important roles in cancer development. These alterations, including DNA hypermethylation and chromatin modifications such as histone methylation and deacetylation,[1] have provided new targets for therapeutic interventions in cancer cells. While advancements have been made in the last decade in the development of inhibitors targeting histone deacetylation or DNA methylation for cancer therapy,[2] there is little progress in the development of histone methylation inhibitors. Aberrant histone methylation, such as histone H3 lysine trimethylation (H3K27me3) induced by oncogenic polycomb protein histone methyltransferase EZH2, has been frequently linked to tumorigenesis,[3] so there has been tremendous effort directed towards the development of small molecules that target EZH2.

We have previously reported the 3-Deazaneplanocin A (DzNep) (Figure 1), an *S*-Adenosylhomocysteine (AdoHcy) hydrolase (SAHH) inhibitor, can effectively deplete the cellular EZH2 complex, inhibit H3K27me3 and other histone methylations and induce robust apoptosis in cancer cells but not in normal cells through the reactivation of many silenced tumour suppressors in cancer cells.[4] Although this compound does not appear to be specific for EZH2-H3K27me3, its anti-cancer activity associated with the depletion of EZH2 has been demonstrated *in vitro* and *in vivo* in many cancer types, including breast, lung, liver, prostate, leukemia.[5] Recent efforts have led to the discovery of a number of selective EZH2 inhibitors e.g. EPZ005687,[6] GSK126,[7] and EI1.[8] However these inhibitors seem to have anti-cancer activity only in B cell lymphomas that carry activating mutations of EZH2, but not in epithelial tumors in which enhanced EZH2 activity is mainly caused by increased gene expression. Intriguingly, a recent study showed that although these inhibitors of EZH2 such as GSK126 have robust activity in the depletion of H3K27me3 in epithelial tumors cells, it has little effect on cancer cell growth.[9] Moreover, a peptide that induces the depletion of EZH2 protein complex is sufficient to inhibit cell growth.[10] This raises a possibility that targeting EZH2 complex, rather than inhibiting H3K27me3, is required for blocking the EZH2-mediated oncogenic effect. Given the remarkable activities of DzNep in the depletion of EZH2 and in the inhibition of tumor growth, we were intrigued with the possibilities of examining DzNep derivatives and analogues so as to enable a better understanding of the structure-activity relationships.

In this study, we report a comprehensive structure-cell based activity study where we screened for DzNep-like activities for the induction of apoptosis in cancer cells. We also report the IC_{50} values of selected DzNep analogues against human SAHH enzymes with the objective of determining if a correlation exists between SAHH inhibition and the ability of the compounds to induce apoptosis.

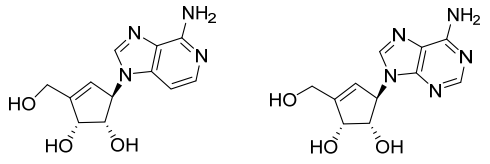

3-Deazaneplanocin (DzNep) Neplanocin (NPA)

Figure 1. Structures of 3-deazaneplanocin A (DzNep) and Neplanocin (NPA)

Results

[a] *Dr. E. K. W. Tam, Dr. T. M. Nguyen, Dr. S. Santhanakrishnan, T. W. Tan, Y. L. Goh, S. Y. Wong, H. Yang, Prof. C. L. L. Chai*
Institute of Chemical and Engineering Sciences, 8 Biomedical Grove, Neuros #07-01, Singapore 138665
E-mail: christina_chai@ices.a-star.edu.sg or phacllc@nus.edu.sg
[b] *C.Z.H. Lim, P. L. Lee, Z. Li, X. Jiang, Dr. Q. Yu*
Cancer Therapeutics and Stratified Oncology, Genome Institute of Singapore, 60 Biopolis Street, #02-01, Singapore138672
Email: yuq@gis.a-star.edu.sg
[c] *E. H.Q. Ong, Dr. J. Hill*
Experimental Therapeutics Centre, 31 Biopolis Way, Nanos Level 3, Singapore 138669
[d] *Department of Pharmacy, 18 Science Drive 4, National University of Singapore, Singapore 117543.*
Supporting information for this article is given via a link at the end of the document.

Synthesis of the target compounds. Our early studies have shown that the natural product, neplanocin A (NPA) (Figure 1) is able to induce the same level of apoptosis as DzNep in our cellular models. We thus designed and synthesized a total of 40 compounds based on variations in the structure of DzNep and NPA (Figure 2). They include (i) variations in the substituents attached to the carbocyclic ring system of NPA (series **A**, compounds **A1**-**A10**),(ii) variations in the carbocyclic ring system (series **B** and **D**, compounds **B1**-**B4**, **D1**-**D19**),(iii) variations in the nature of the heterocyclic ring attached to the carbocyclic ring (series **C**, compounds **C1**-**C9**). Only the synthesis of selected compounds are discussed here. The full experimental details on the synthesis of the target compounds can be found in the Supporting Information.

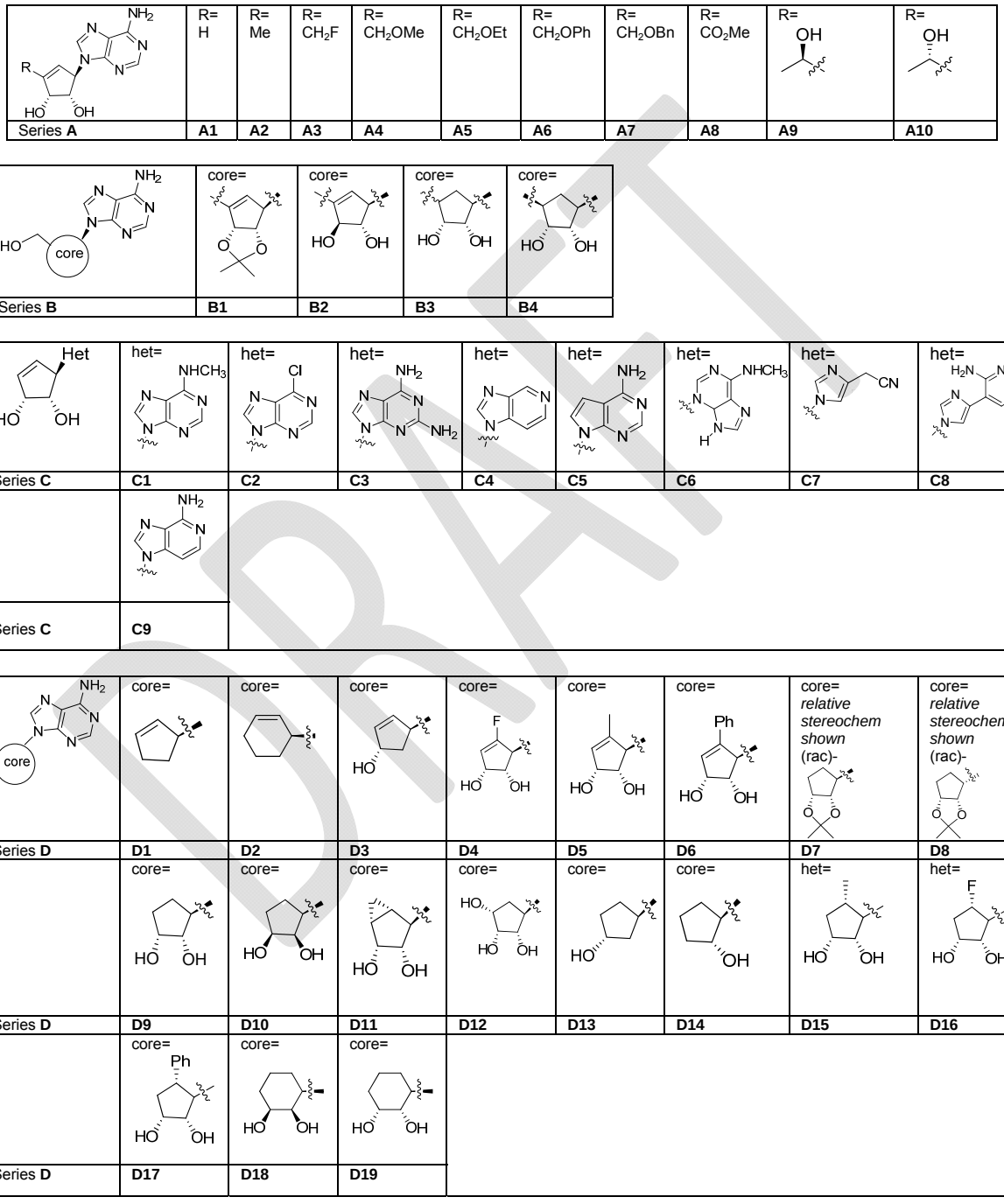

Figure 2. List of compounds for structure-cell activity determination

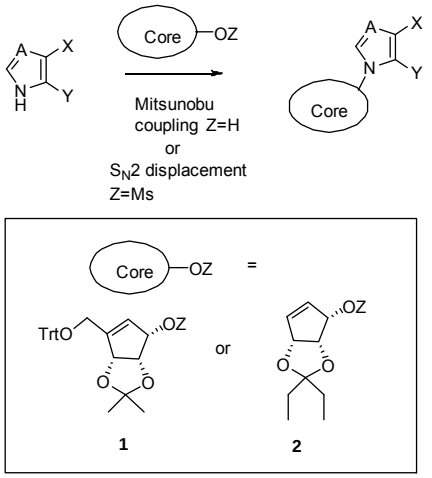

Scheme 1. Key coupling step to target compounds

In general, the target compounds were synthesized by reacting the carbocyclic scaffold ('core') with the appropriate hetereocyclic bases under Mitsunobu or S_N2 conditions (Scheme 1).

For compounds in series **A** and **C**, the core comprised of functionalized cyclopentene **1** and **2** while that in the series **B** and **D** were either commercially available or were synthesized following literature procedures (see Supporting Information).

The cyclopentenol **1** (Z = H) was synthesized in 8 steps starting from D-ribose,[11] and subsequent transformations gave the protected NPA **3** in good yields. With protected NPA in hand, protected precursors of **A2-A10** were accessed from the advanced intermediate **3** as summarized in Scheme 2. Compound **4** was directly accessed from **3** through the reaction of the alcohol with 1,1'-thiocarbonyl diimidazole, and tributyltin hydride, while the synthesis of **5** was achieved using dimethylaminosulfur trifluoride (DAST). Methylation, ethylation and benzylation of **3** gave the *O*-analogues **6**, **7** and **9** respectively. The phenoxy derivative **8** was obtained under Mitsunobu conditions while the methyl ester **10** was accessed *via* a three step procedure (oxidation to the aldehyde with Dess-Martin periodinane, followed by oxidation to the acid and esterification) from the alcohol **3**. Compounds **11** and **12** were derived from the aldehyde followed by treatment with methyl magnesium iodide. In all of the cases, global deprotection of the Boc and acetonide protecting groups under acidic conditions afforded the target compounds.

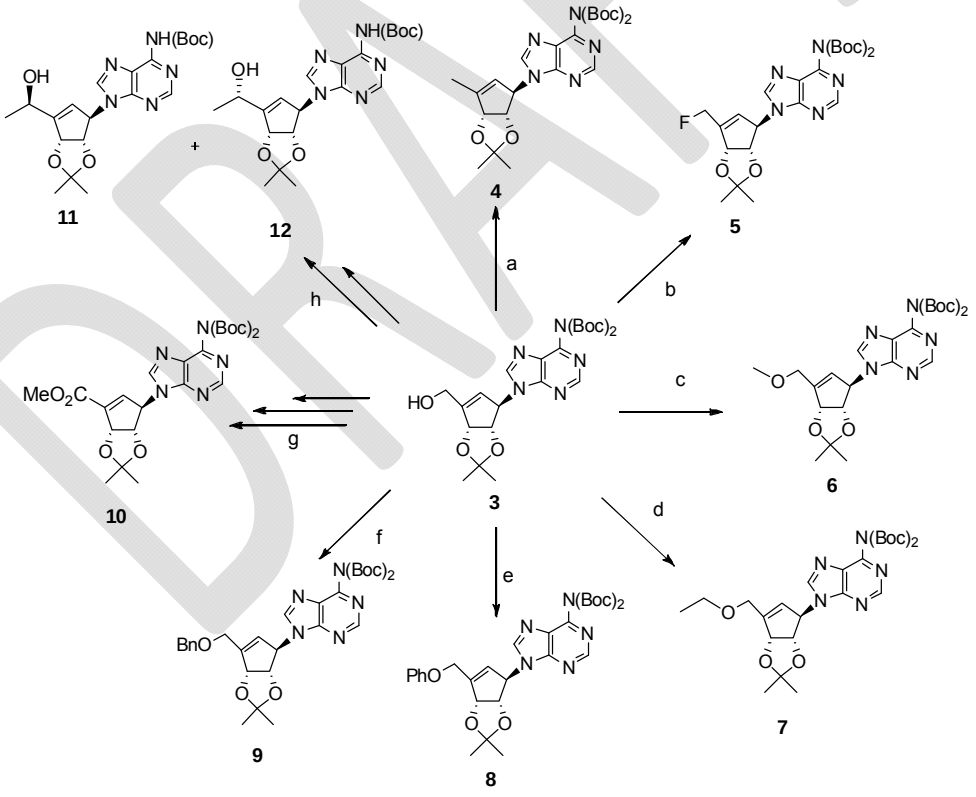

Scheme 2. Reagents and conditions (a) 1,1'-thiocarbonyl diimidazole, tributyltinhydride, 68%; (b) DAST, 72%; (c) MeI, NaH, DMF, rt, 16 h, 54%; (d) EtI, NaH, DMF, rt, 16 h, 25%; (e) PhOH, PPh_3, DIAD, THF, rt, 18 h, 78%; (f) BnBr, NaH, DMF, rt, 16 h, 39%; (g) (i) Dess-Martin periodinane, DCM, 95% (ii) Oxone™, DMF, rt, 48 h, 74% (iii) (Trimethylsilyl)diazomethane, MeOH-toluene, rt, 48 h, 47%; (h) (i) Dess-Martin periodinane, DCM, 95% (ii) MeMgBr, THF, 16 h, 86%.

For the synthesis of cyclopentenol **15**, D-ribose was converted, through a sequence of reactions, to a diastereomeric mixture of dienes **13** following modified procedures (Scheme 3).[12] Ring closing metathesis followed by PCC oxidation gave the enone **14** in reasonable yields. The ketone functionality of the enone was then reduced under Luche's conditions to afford a single stereoisomer **15** in high isolated yields.

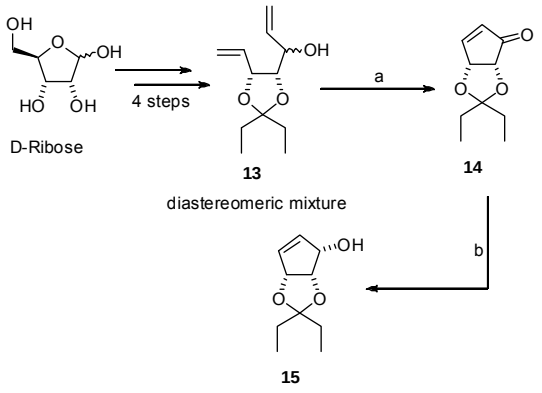

Scheme 3. Reagents and conditions (a) (i) RCM (ii) pyridinium chlorochromate (b) $NaBH_4$, $CeCl_3$, 85-95%

With this alcohol **15** in hand, coupling with *N*,*N*-diprotected adenine, followed by deprotection gave compound **A1** in good yields (Scheme 4). Subsequent hydrogenation of **A1** gave compound **D9** in quantitative yields.

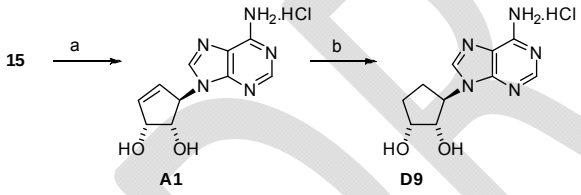

Scheme 4. Reagents and conditions (a) (i) PPh_3, DIAD, diBoc adenine, THF, 80% (ii) 10% HCl in 1:1 H_2O/MeOH mixture, 90%. (b) H_2, 10% Pd/C in H_2O, rt, overnight, quant.

The synthesis of **D4** and **D16** are summarized in Scheme 5. Using enone **14** as described in Scheme 4, iodination followed by reduction of ketone **16** provided alcohol **17** in good yields. The free hydroxyl group of **17** was protected as its *tert*-butyldiphenylsilyl (TBDPS) ether **18**. Fluorination of iodo-alkene **18** with excess *N*-fluorobenzenesulfonimide (NFSI) and BuLi furnished an inseparable mixture of compounds **19** and **20** in a ratio of 3:1, which was used as is in the subsequent steps. Deprotection of the TBDPS groups of the mixture of **19** and **20** using tetrabutylammonium fluoride (TBAF) provided an inseparable mixture of alcohols. Tosylation of the mixture to give **21** and **22**, followed by alkylation with adenine in DMF, yielded a mixture of **23** and **24**, which was separable by column chromatography. The reduction of the double bond of **23** in the presence of Pd/C under high pressure (50 psi) provided **25** in 73% yield. The stereochemistry of the fluorine substituent and the basic skeleton of **25** was unambiguously characterized by X-ray crystallography (see Supporting Information). Hydrolysis of **25** in acidic medium gave **D16** in good yields. Similarly, hydrolysis of **23** furnished **D4** in good yields.

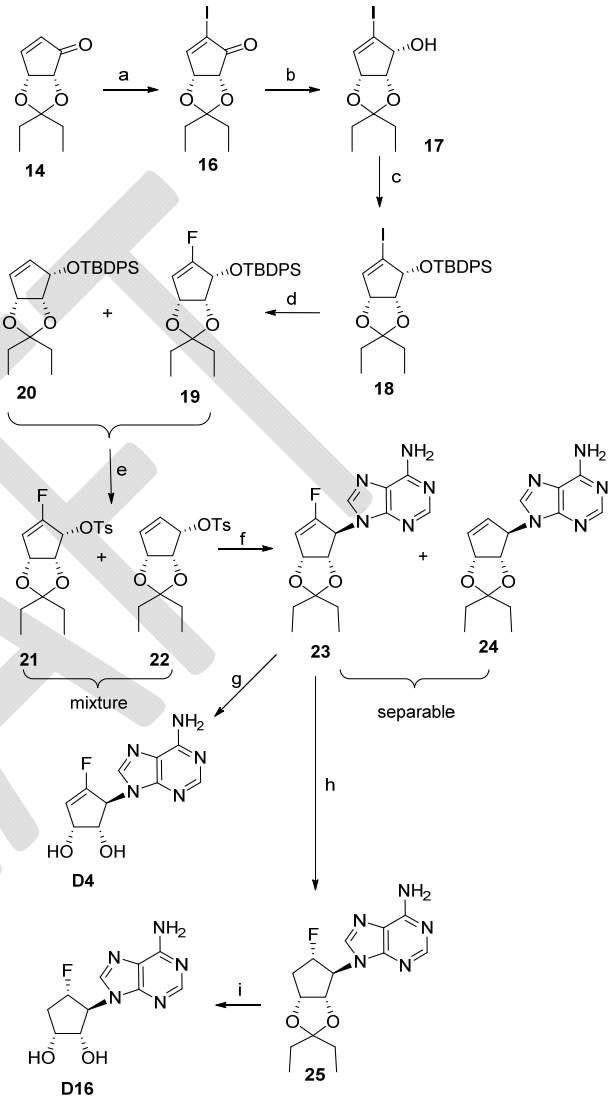

Scheme 5. Reagents and conditions (a) I_2, pyridine, 10:1 DCM/THF, rt, 75%; (b) $NaBH_4$, $CeCl_3$, MeOH, 98%; (c) TBDPS, imidazole, 10:1 DCM/THF, rt, 83%; (d) *n*-BuLi, NFSI, -60 °C, THF; (e) (i) TBAF, THF (ii) TsCl, NEt_3, DMAP, DCM; (f) adenine, NaH, 80 °C, DMF, 28% over 4 steps for **23**; (g) 2 N HCl, rt, 48 h, 79%; (h) 10% Pd/C, H_2 (50 psi), MeOH, rt, 73%; (i) 2 N HCl, rt, 48 h, 95%

Compounds **D5**, **D6**, **D15** and **D17** were synthesized from the versatile iodocyclopentene **17** and **18** through palladium catalyzed reactions followed by a sequence of transformations similar to that described previously (see Supporting Information for details). The stereochemistry of the newly generated

stereocenters in compounds **D15** and **D17** are presumed to be *syn* to the hydroxyl groups of the cyclopentane ring by analogy to the observation made with **D16**.

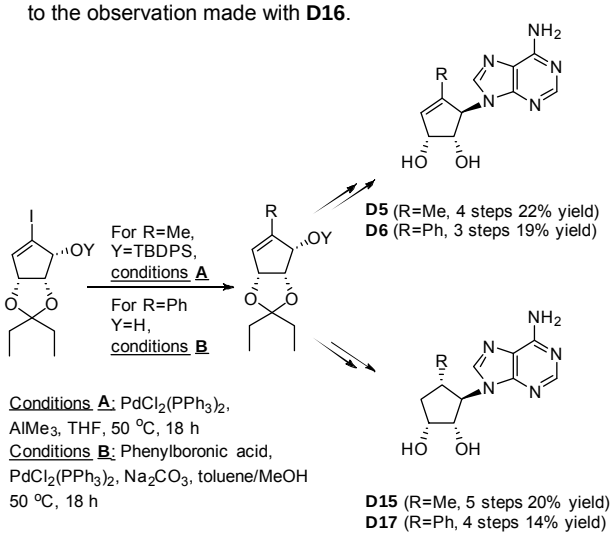

Scheme 6. Synthetic routes to **D5**, **D6**, **D15** and **D17**.

Structure-cell based activity studies. We have previously shown that DzNep is able to synergize with histone deacetylase (HDAC) inhibitor, Trichostatin A (TSA), to induce robust apoptosis in colon cancer DLD1 cells.[13] We also showed that DzNep induces strong apoptosis upon the activation of transcription factor E2F1 in colon cancer cell HCT116.[14] We thus used these two independent *in vitro* cellular systems to determine the cellular activities of DzNep-like compounds. We first started with DLD1 cells to screen for DzNep analogs that can increase apoptosis in combination with TSA. DLD1 cells were treated with 5 μM DzNep analogs for 48 h followed by 150 nM HDACi, TSA, for additional 24 h before harvesting for apoptosis assessment through FACS analysis of DNA content. The positive hits were compounds that show increased apoptotic cell death on drug combination, i.e., the apoptotic cell death is greater than the sum of that caused by DzNep analog or TSA alone. The results are summarized in the Supporting Information. From the screening studies, the effect of substitution (R) at the C-4 position of the carbocyclic ring of NPA was investigated. Positive hits are compounds **A1**-**A4**, **A9** and **A10** (i.e. compounds possessing H, Me, CH_2F, CH_2OMe, $CH(OH)CH_3$ substituents instead of the CH_2OH substituent present in NPA). Replacement of the carbocyclic ring of NPA with other carbocyclic core structures (series **B**) indicated that the free hydroxyl substituents are critical for DzNep-like apoptotic activity as is the stereochemistry of the hydroxyl groups as **B1** and **B2** do not show any synergistic activity. Surprisingly, saturation of the double bond (cyclopentane versus cyclopentene, compound **B3**) retained the synergistic apoptotic activity.

In view of the simplicity of the structure of **A1**, further structural modifications were centered on variations of this structure. Compounds in series **C** examined the effect of varying the heterocyclic bases and in all the compounds tested in this series, none show any significant DzNep-like apoptotic activity. Series **D** further examined the effect of varying the carbocyclic core. Consistent with the observations made previously, saturation of the double bond of **A1** (compound **D9**) retained the apoptotic activity. The vinyl fluoride **D4** and the saturated compound **D16** showed synergistic apoptotic cell death while all other variations of the carbocyclic core resulted in loss of apoptotic activity. This indicates the sensitivity of the carbocyclic core in inducing apoptosis. As observed with compounds in Series **B**, the location, stereochemistry and presence of both the secondary hydroxyl groups are critical for apoptosis. In addition, the ring size is also important. From these studies, three compounds **D4**, **D9**, **D16** have been identified as showing comparable synergistic apoptotic activity as DzNep.

A secondary screen with selected positive hits were carried out with HCT116 cells in which E2F1 is fused to the 4-hydroxytamoxifen (4-OHT)-responsive ligand-binding domain of the estrogen receptor (ER) to form an ER-E2F1 fusion protein and becomes activated after addition of 4-OHT. We have previously shown that DzNep, upon addition of 4-OHT (to activate E2F1) in the cell culture, induced strong apoptosis in this system, while only a modest level of apoptosis was induced in the absence of 4-OHT.

As shown in Figure 3, in HCT116 ER-E2F1 cells, 4-OHT and DzNep alone induced approximately 13% and 20% of cells in apoptosis, respectively, as determined by cells in sub-G1 in FACS analysis, while the combination of 4-OHT and DZNep, resulted in 54% of cells in apoptosis. The compounds **A4**, **D4**, **D9** and **D16** exhibited comparable activities to DzNep, resulting in synergistic apoptosis of 45%, 47%, 49% and 47%, respectively when combined with 4-OHT.

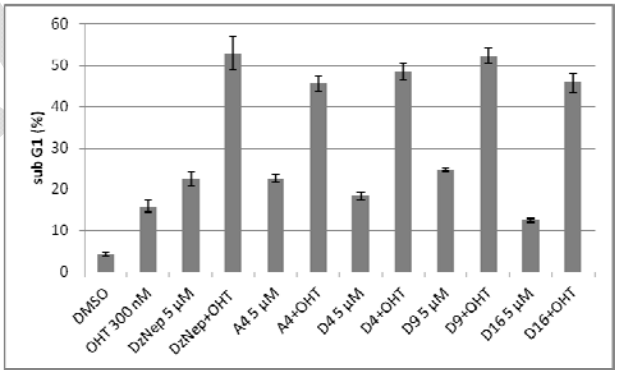

Figure 3. *In vitro* assessment of DzNep analogs. p53-null HCT116-ER-E2F1-expressing cells were treated with 5 μM DzNep or DzNep analogs including **A4**, **D4**, **D9** or **D16** in the presence or absence of 300 nM 4-OHT. After 72 h, cells were harvested, and cell death was assessed by PI staining using FACS.

We also show that the DzNep analogs have the capacity to deplete histone methylations including H3K27me3, H3K4me3 and H3K20me3, though **D9** seems to be more selective on H3K27me3 as shown in Figure 4.

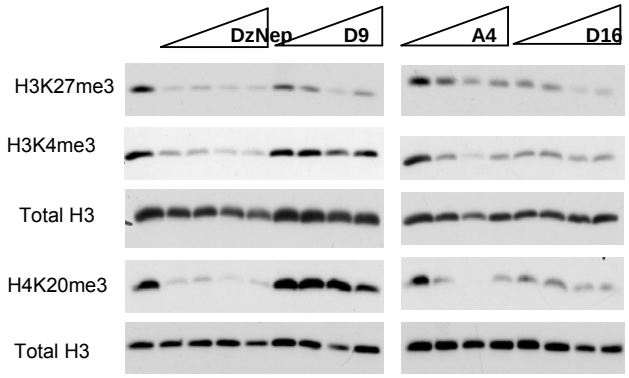

Figure 4. Western blot showing the effect of DzNep analogs on histone methylations. HCT116 cells were treated with increasing concentrations of indicated compounds (0.5, 1, 2.5 and 5 μM) for 72 hrs before harvested for western blot analysis.

S-Adenosylhomocysteine Hydrolase (SAHH) inhibition of selected compounds. A total of 16 compounds (DzNep, NPA, **A1**, **A3**-**A6**, **A9**-**10**, **D5**-**6**, **D9**, **D15**-**17**) were tested for inhibition of human SAHH. Although the IC_{50} or K_i values of some of these compounds have already been reported in the literature, comparison of the literature values proved to be difficult due to the different assay platforms and the species and form (recombinant or purified native) of SAHH used. A summary of the results is shown in Table 1. From these studies, it is noted that NPA and DzNep are potent inhibitors of SAHH, while **D9** is approximately 6 fold less potent than DzNep. Interestingly **D16** was 18 fold less potent than **D9**, while the activity of **D4** and **D16** are similar. The ranking of the compounds in terms of the IC_{50} values with SAHH inhibition is NPA (most potent)> **A3** > DzNep > **D9** > **A9~A4** > **A10** > **A6** > **A5** > **D17** > **D16~D4~D15** > **A1** > **D5~D6** (least potent).

In vitro ADME and hERG studies. Compounds **D9** and **D16** were selected for *in vitro* ADME evaluation and hERG studies. Measurement of the log D values showed that both compounds have comparable log D values (-1.6 at pH 3.0 and -0.5 at pH 7.4). In addition, the solubilities of the two compounds at pH 2 and 6.5 did not change and is at *ca*. 300 μM. The half-lives of the compounds with Human Liver Microsomes were measured to be 2636 min and 1029 min respectively, while that with Male Rat Liver Microsomes and Male Mouse Liver Microsomes were 183 min and 307 min for **D9** and 836 and 982 min for **D16** respectively. In terms of hERG safety studies, the IC_{50} values of both **D9** and **D16** were greater than 100μM using the FluxOR hERG Fluorescence Assay while using the electrophysiological hERG test, the IC_{50} of both of these compounds were greater than 10μM. From these data, it can be concluded that both **D9** and **D16** do not show significant inhibition of the hERG channel.

The anti-tumor effects of D9 in HCT116 tumor xenograft mouse model. To evaluate the anti-cancer effect of **D9** *in vivo*, HCT-116 subcutaneous xenograft tumor mouse model was used. In this model, 5 x 10^6 of HCT116 cells were injected into Balb/c nude mice subcutaneously (s.c.) and when the tumors reached an average of 200 mm m^3 in size, **D9** was administered through intraperitoneal (i.p.) injection. As shown in Figure 4, **D9** administration at 30 or 80 mg/kg 5 days a week for two weeks resulted in marked decrease in tumor growth in a dose-dependent manner. During the course of drug treatments, the body weight of mice was monitored daily. **D9** did not give rise to obvious signs of toxicity and only a minimum loss of body weight was observed (Figure 5). These data suggest that **D9** has significant anti-tumor effects while at the effective doses it is well tolerated in the recipient mice (Figure 5). The pharmacokinetic profile of **D9** in Sprague-Dawley rats through PO administration (5 mg/kg) also suggested that **D9** is readily absorbed and has a half-life of 5 h.

a.

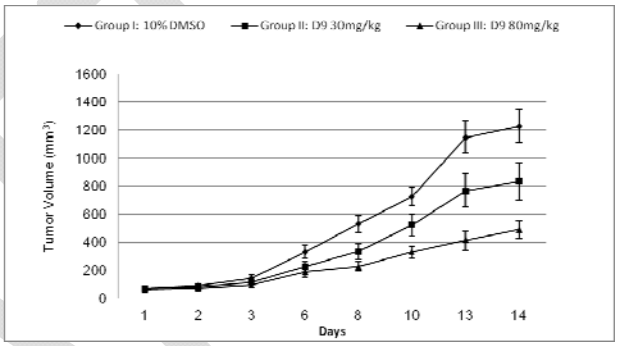

b.

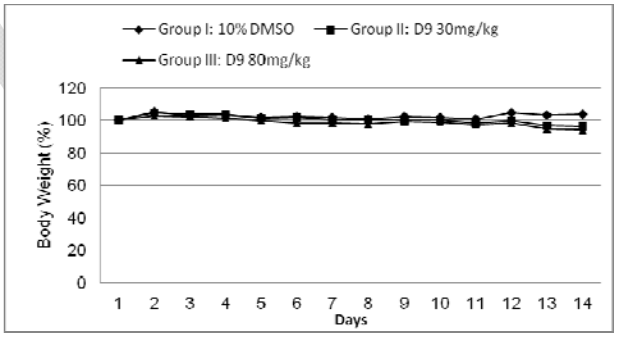

Figure 5. Effects of **D9** *in vivo*. (a) effect of **D9** on HCT116 Xenograft tumor growth. (b) the effect of **D9** on body weight change of mice.

Discussion

Our studies above have delineated some of the critical structural features required for DzNep-like apoptotic activity (Figure 6). In brief, the structure-cell activity relationship identifies that the 2,3-dihydroxycarbocyclic core of DzNep, can be saturated or unsaturated, is needed for synergistic activity (Figure 6). The heterocyclic base at the C1 position of the carbocycle can either be adenine or deazaadenine but all the other heterocyclic

combinations tested led to loss in activity. Thus compound **A1** and **D9** contain the minimum pharmacophore required for synergistic apoptotic activity. When considering the SAR of DzNep and NPA, it is apparent that variation in the substituents at the C-4 position cannot be easily rationalized. The presence of a substituent is not necessary for synergistic apoptotic activity as seen with compound **A1**. There is also some tolerance for small substituents at the C-4 position of the carbocyclic ring. Interestingly, a secondary alcohol at the C-4 position does not lead to large losses in biological activity. The presence of substituents at the C-5 position of the carbocyclic ring causes large losses in synergistic apoptotic activity - the exception is when a fluorine atom replaces the hydrogen atom at C-5 of **A1** and **D9**.

SAHH is an important enzyme that catalyses the hydrolysis of *S*-adenosylhomocysteine (AdoHcy) to adenosine and *L*-homocysteine.[15] Accumulation of AdoHcy through inhibition of SAHH can in turn lead to inhibition of methyltransferases and thus indirectly affect the epigenetic mechanisms of a cell. DzNep and NPA have long been recognized as potent inhibitors of SAHH. Indeed early studies have focused on the development of these and related compounds as anti-virals through the inhibition of SAHH.[16] The mechanisms of SAHH inhibition are suggested to either occur *via* a reversible Type I mechanism via inactivation of the enzyme through the oxidation of the cofactor NAD+ to NADH, or *via* an irreversible Type II mechanism via covalent binding of inhibitor with a nucleophilic residue at the active site.[17] Of the selection of the target compounds measured for SAHH activity, we note that the most potent SAHH inhibitor was NPA (IC_{50} at 40 nM), followed by the fluorinated compound **A3** (IC_{50} =130 nM), then DzNep at (IC_{50} = 230 nM). We note that these values for NPA and DzNep differ from that reported in the literature for human SAHH.[16b, 18] The compounds that were tested from series **A** showed that SAHH inhibition is sensitive to modifications of the substituents at the C-4 position. The stereoisomers of the secondary alcohol **A9** showed a 1.5 fold difference in SAHH activities as compared to the enriched mixture of **A10** (contains 15% **A9**). From the literature, a large difference in SAHH activities between **A9** and **A10** was reported, in favour of **A9**, as measured with rabbit SAHH.[19] For the selected compounds studied in series **D**, the most potent compound is **D9** which showed very different activity in comparison with the unsaturated compound **A1**. The vinyl fluoride **D4** was the best compound amongst the unsaturated compounds in series **D** and **D4** has been reported to inhibit SAHH *via* the Type II mechanism.[20] The saturated compounds **D15**-**D17** have comparable SAHH activity. Our SAHH studies identified NPA, DzNep, methyl ether **A4**, the fluorinated **A3**, alcohol **A9** and **D9** as the best inhibitors of SAHH. Broadly speaking, these compounds are also potent inducers of apoptosis. However there is no discernible direct relationship between SAHH inhibition and synergistic apoptotic activities. Specifically compounds (e.g. **D15**) that have reasonable SAHH inhibitory activities do not display synergistic apoptotic activity.

Conclusion

The toxicities and the short half-lives of DzNep and NPA have long been realized and this is in part due the rapid phosphorylation by adenosine kinase. [20] Through these studies, we have identified two compounds that show a longer half-life than NPA and DzNep. In addition, animal studies with **D9** show that it has lower toxicity than DzNep and is effective in shrinking tumors. Thus we have successfully identified *at least* two compounds that are potentially superior to DzNep and NPA for further development as chemotherapeutics for epigenetic therapy. Further future mechanistic studies will undoubtedly shed more information on the mode of action of these compounds.

Table 1. IC_{50} (μM) value determination using enzyme assay with recombinant expressed human SAHH.

Structure	IC_{50} values (μM)	Structure	IC_{50} values (μM)
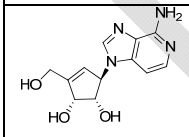 **DzNep**	0.23±0.07 [Lit: K_i=23 nM, human SAHH] [25]	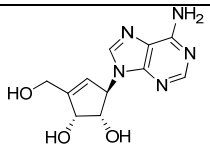 **NPA**	0.04±0.01 [Lit: IC_{50}=0.82 μM, human SAHH] [26]
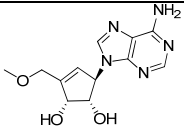 **A4**	2.22±0.24 [Lit: IC_{50} >10 μg/mL, rabbit erythrocyte] [27]	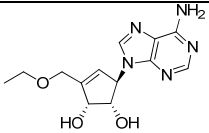 **A5**	13.1*
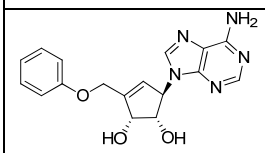 **A6**	7.47±4.30	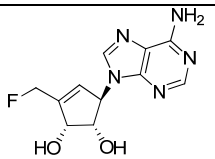 **A3**	0.13±0.04 [Lit: IC_{50} >10 μg/mL, rabbit erythrocyte] [27]

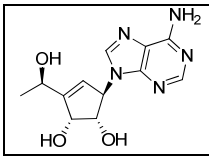 **A9**	1.71±0.24 [Lit: IC_{50}=0.2 μg/mL, rabbit erythrocyte] [27]	Tested as a mixture of **A9** and **A10** in the ratio of 15:85.	3.46±0.87
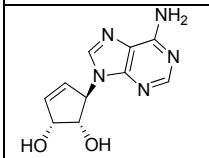 **A1**	44.59±13.34 [Lit: K_i=35 nM, bovine liver] [28]	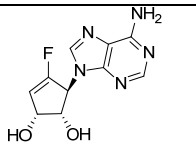 **D4**	24.39±0.40
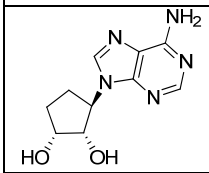 **D9**	1.35±0.35 [Lit: IC_{50}=9 μM, human SAHH] [29]	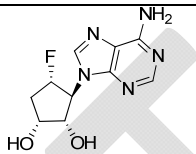 **D16**	25.18±2.17
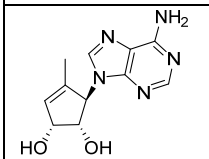 **D5**	>200	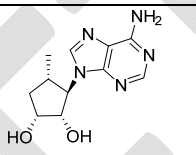 **D15**	25.7*
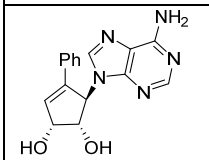 **D6**	>200	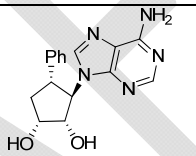 **D17**	20.9*

All experiments were carried out in triplicates using two independent runs unless specified otherwise. (*) indicates only a single run.

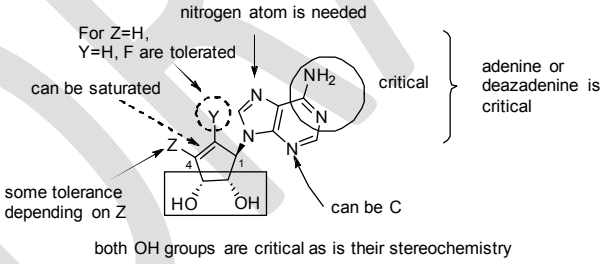

Figure 6. Critical structural features for DzNep like-apoptotic activity

Experimental Section

Chemistry. Unless otherwise specified, materials were purchased from commercial suppliers and used without further purification. Solvents for reactions were taken from a Glass contour solvent purification system under nitrogen. ^{1}H NMR and ^{13}C NMR spectra were acquired on a Bruker 400. UltraShield Spectrometer operating at 400 MHz and 100 MHz respectively, unless specified otherwise. All the proton spectra were referenced to the respective residual solvent peaks (CD_3OD: 3.31; DMSO-d_6: 2.50; D_2O: 4.79 ppm) except for those recorded in $CDCl_3$ were referenced to TMS or residual solvent peak at 7.26 ppm. Carbon spectra were referenced to the central peak of the respective residual solvents (CD_3OD: 49.0; DMSO-d_6: 39.5; $CDCl_3$: 77.2 ppm). Where necessary, the signals of novel compounds were assigned by 1D NOE differences and/or 2D NMR techniques: ^{1}H-^{1}H COSY, ^{13}C-^{1}H HMQC, and ^{13}C-^{1}H HMBC. These experiments were performed using standard Bruker microprograms. Low-resolution and high-resolution electron impact mass spectra (EIMS) were measured using a Finnigan MAT95XP double-focusing mass spectrometer. Low-resolution electrospray ionization (ESI) mass spectra were recorded using Waters Quattro Micro™ API, and high resolution mass spectra were obtained using the Agilent 6210 Time-of-Flight LC/MS. Flash column chromatographies were conducted manually using silica gel 60 Merck (35-70 µm) with an overpressure of 200 mbars. Amination reactions using 33% aqueous ammonia were carried out using a high pressure reactor. Elemental analysis was performed using a EuroEA3000 series CHNS Analyzer.

Compounds **B1**,[22] **B2**,[23] **D12**,[24] were synthesized following literature procedures while **B4** is commercially available. Detailed procedures and characterization data for all other compounds are provided in the Supporting Information.

Biology.

***In vitro* assessment of DzNep analogs.** p53 Knock out (KO) HCT116 cells that express inducible E2F1 (ER-E2F1) were used to assess the ability of DzNep analogs to induce E2F1-dependent apoptosis.[14] To activate E2F1, 300 nM 4-hydroxytamoxifen (4-OHT) were added to the tissue culture medium. Cell apoptosis induced by DzNep analogs were measured in the presence or absence of 4-OHT for 72 hours by Flow Cytometric Analysis of DNA content. To measure the ability of DzNep analogs to synergize with histone deacetylase (HDAC) inhibitor (HDACi) for apoptosis induction, DLD1 cells were treated with 5 µM DzNep analogs for 48 hours followed by 150 nM HDACi Trichostatin A (TSA) for additional 24 hours before harvested for FACS analysis of DNA content. To assess the apoptosis induction, cells were harvested and fixed in 70% ethanol. Fixed cells were stained with propidium iodide (50µg/ml) after treatment with RNase (100 µg/ml). The stained cells were analyzed for DNA content by fluorescence-activated cell sorting (FACS) in a FACScalibur (Becton Dickinson Instrument, San Jose, CA). Cell cycle fractions were quantified using the CellQuest software (Becton Dickinson). Apoptosis was determined by measuring the DNA content of cells in sub-G1.

***In vivo* anti-tumor assessment of DzNep analogs.** The female athymice BALB/c nude mice (5-8 week-old) were housed in the Biological Resource Centre. Mice were implanted subcutaneously in flank with 5 × 10^6 cells of HCT-116 parental human colon carcinoma. When tumors reached ~ 200 mm^3, the mice were divided four groups (10 mice per group) and were treated with vehicle or DzNep analog **D9** at 30 and 80 mg/kg by intraperitoneal (IP) injection for 14 days. Tumor growth and the whole body weight changes of mice were monitored every other day. All animal studies were conducted in compliance with animal protocols approved by the A-STAR-Biopolis Institutional Animal Care and Use Committee (IACUC) of Singapore.

Statistical Analysis. A student's t-test is used to determine the statistical significance of tumor volumes and body weight changes between groups. Statistical analyses are conducted at a *p* level of 0.05. SPSS was used for all statistical analyses and graphic presentations.

Production and purification of recombinant SAHH. The GST-tagged SAHH in the pDEST 565 vector was expressed in Escherichia coli BL21 (DE3) pLysS and inoculated overnight in LB medium with 34 µg/mL chloramphenicol and 100 µg/mL ampicillin at 37 °C with orbital shaking at 200 rpm. The culture was then diluted 1:250 in LB with chloramphenicol and ampicillin and maintained at 30 °C until the OD600 value reached 0.5-0.6 arbitrary units. After the addition of 400 µM isopropyl-β-D-1-thiogalactopyranoside, the culture was incubated for an additional 16 h. The bacterial pellet was then collected by centrifugation and lysed by sonication in buffer containing 10 mM sodium phosphate, 150 mM NaCl, 5 ug/mL DNAseI, 0.625 mg/mL Lysozyme, 1X protease inhibitor (pH = 7.4) with 5 mM 2-mecaptoethanol. The overexpressed protein was purified using the Bio-Scale Mini Profinity GST 5 mL cartridges (BioRad) followed by concentration and desalting in 100 mM Tris Buffer, 100 mL NaCl (pH = 8.0). The concentrated SAHH-GST is cleaved with Tobacco Etch Virus (TEV) protease at 1 µg TEV per 50 µg GST-tagged protein in 20 mM Tris (pH = 8.0), 100 mL NaCl and 2 mM DTT buffer. The cleaved GST is removed using Glutathione Sepharose 4B Beads (GE Healthcare) after 1 h incubation in 10 mM Tris, 50 mM NaCl (pH = 7.5).

SAHH Activity Assay. The thiol group containing products of the SAHH catalyzed reaction were detected in a 96-well format through the florescent thiol detection reagent, ThioGlo1 (Calbiochem). 5 µL of freshly prepared SAHH (100 ng/µL in 100 mM Tris pH =7.5) were added to 5 µL Inhibitor/ DMSO control, 15 µL of freshly prepared assay buffer (3 µM DTT, 150 µM NAD, 3 mM EDTA), 15 µL of 100 mM Tris (pH =7.5) and incubated at 37 °C for 30 min. After incubation, 5 µL of 750 µM SAH (Sigma, freshly prepared in 100 mM Tris, pH =7.5) was added and further incubated at 37 °C for 10 min. 500 µM ThioGlo1 freshly diluted in 100 mM Tris (pH =7.5) were added and incubated at 37 °C for another 15 min. The florescence signal is detected by Safire2 (Tecan) with a 380 nM excitation and 510 nM emission filter. IC_{50} (concentration of an inhibitor where the response is reduced by half) measurements were performed using GraphPad Prism Version 5.00 for Windows (Graphpad software, San Diego California USA).

Acknowledgements

The authors thank the Agency for Science Technology and Research (A*STAR) (CCOG01-001-2008 and ETPL/10-FS0002) for the financial support of this project.

Keywords: epigenetics• deazaneplanocin A • neplanocin A • structure-cell-activity relationships • SAHH

[1] K. Helin and D. Dhanak, *Nature* **2013**, *502*, 480-488.

[2] a) J. S. Garcia, N. Jain and L. A. Godley, *Onco. Targets Ther.* **2010**, *3*, 1-13; b) O. A. O'Connor, M. L. Heaney, L. Schwartz, S. Richardson, R. Willim, B. MacGregor-Cortelli, T. Curly, C. Moskowitz, C. Portlock, S. Horwitz, A. D. Zelenetz, S. Frankel, V. Richon, P. Marks and W. K.

Kelly, *J. Clin. Oncol.* **2006**, *24*, 166-173; c) R. L. Piekarz, R. Frye, M. Turner, J. J. Wright, S. L. Allen, M. H. Kirschbaum, J. Zain, H. M. Prince, J. P. Leonard, L. J. Geskin, C. Reeder, D. Joske, W. D. Figg, E. R. Gardner, S. M. Steinberg, E. S. Jaffe, M. Stetler-Stevenson, S. Lade, A. T. Fojo and S. E. Bates, *J. Clin. Oncol.* **2009**, *27*, 5410-5417.

[3] a) F. Crea, L. Fornaro, G. Bocci, L. Sun, W. L. Farrar, A. Falcone and R. Danesi, *Cancer Metastasis Rev.* **2012**, *31*, 753-761; b) F. Crea, E. M. Hurt, L. A. Mathews, S. M. Cabarcas, L. Sun, V. E. Marquez, R. Danesi and W. L. Farrar, *Mol. Cancer* **2011**, *10*, 40; c) J. A. Simon and C. A. Lange, *Mutat. Res.* **2008**, *647*, 21-29.

[4] J. Tan, X. Yang, L. Zhuang, X. Jiang, W. Chen, P. L. Lee, R. K. Karuturi, P. B. Tan, E. T. Liu and Q. Yu, *Genes Dev.* **2007**, *21*, 1050-1063.

[5] a) T. Chiba, E. Suzuki, M. Negishi, A. Saraya, S. Miyagi, T. Konuma, S. Tanaka, M. Tada, F. Kanai, F. Imazeki, A. Iwama and O. Yokosuka, *Int. J. Cancer* **2012**, *130*, 2557-2567; b) A. Hayden, P. W. Johnson, G. Packham and S. J. Crabb, *Breast Cancer Res. Treat.* **2011**, *127*, 109-119; c) J. K. Lee and K. C. Kim, *Biochem. Biophys. Res. Commun.* **2013**, *438*, 647-652; d) J. Zhou, C. Bi, L. L. Cheong, S. Mahara, S. C. Liu, K. G. Tay, T. L. Koh, Q. Yu and W. J. Chng, *Blood* **2011**, *118*, 2830-2839.

[6] S. K. Knutson, T. J. Wigle, N. M. Warholic, C. J. Sneeringer, C. J. Allain, C. R. Klaus, J. D. Sacks, A. Raimondi, C. R. Majer, J. Song, M. P. Scott, L. Jin, J. J. Smith, E. J. Olhava, R. Chesworth, M. P. Moyer, V. M. Richon, R. A. Copeland, H. Keilhack, R. M. Pollock and K. W. Kuntz, *Nat. Chem. Biol.* **2012**, *8*, 890-896.

[7] M. T. McCabe, H. M. Ott, G. Ganji, S. Korenchuk, C. Thompson, G. S. Van Aller, Y. Liu, A. P. Graves, A. Della Pietra, 3rd, E. Diaz, L. V. LaFrance, M. Mellinger, C. Duquenne, X. Tian, R. G. Kruger, C. F. McHugh, M. Brandt, W. H. Miller, D. Dhanak, S. K. Verma, P. J. Tummino and C. L. Creasy, *Nature* **2012**, *492*, 108-112.

[8] W. Qi, H. Chan, L. Teng, L. Li, S. Chuai, R. Zhang, J. Zeng, M. Li, H. Fan, Y. Lin, J. Gu, O. Ardayfio, J. H. Zhang, X. Yan, J. Fang, Y. Mi, M. Zhang, T. Zhou, G. Feng, Z. Chen, G. Li, T. Yang, K. Zhao, X. Liu, Z. Yu, C. X. Lu, P. Atadja and E. Li, *Proc. Natl. Acad. Sci. USA* **2012**, *109*, 21360-21365.

[9] Z. N. Wee, Z. Li, P. L. Lee, S. T. Lee, Y. P. Lim and Q. Yu, *Cell Rep* **2014**.

[10] W. Kim, G. H. Bird, T. Neff, G. Guo, M. A. Kerenyi, L. D. Walensky and S. H. Orkin, *Nat. Chem. Biol.* **2013**, *9*, 643-650.

[11] a) J. H. Cho, D. L. Bernard, R. W. Sidwell, E. R. Kern and C. K. Chu, *J. Med. Chem.* **2006**, *49*, 1140-1148; b) B. Y. Michel and P. Strazewski, *Tetrahedron* **2007**, *63*, 9836-9841.

[12] H. Osato, I. L. Jones, A. Chen and C. L. L. Chai, *Org. Lett.* **2010**, *12*, 60-63.

[13] X. Jiang, J. Tan, J. Li, S. Kivimae, X. Yang, L. Zhuang, P. L. Lee, M. T. Chan, L. W. Stanton, E. T. Liu, B. N. Cheyette and Q. Yu, *Cancer Cell* **2008**, *13*, 529-541.

[14] Y. Zhao, J. Tan, L. Zhuang, X. Jiang, E. T. Liu and Q. Yu, *Proc. Natl. Acad. Sci. USA* **2005**, *102*, 16090-16095.

[15] M. A. Turner, X. D. Yang, D. Yin, K. Kuczera, R. T. Borchardt and P. L. Howell, *Cell Biochem. Biophys.* **2000**, *33*, 101-125.

[16] a) P. K. Chiang, *Pharmacol. Ther.* **1998**, *77*, 115-134; b) E. De Clercq, *Nucleosides Nucleotides Nucleic Acids* **2005**, *24*, 1395-1415; c) C. K. Tseng, V. E. Marquez, R. W. Fuller, B. M. Goldstein, D. R. Haines, H. McPherson, J. L. Parsons, W. M. Shannon, G. Arnett, M. Hollingshead and et al., *J. Med. Chem.* **1989**, *32*, 1442-1446.

[17] M. S. Wolfe and R. T. Borchardt, *J. Med. Chem.* **1991**, *34*, 1521-1530.

[18] M. Bray, J. Driscoll and J. W. Huggins, *Antiviral Res.* **2000**, *45*, 135-147.

[19] S. Shuto, T. Obara, M. Toriya, M. Hosoya, R. Snoeck, G. Andrei, J. Balzarini and E. Declercq, *J. Med. Chem.* **1992**, *35*, 324-331.

[20] H.O. Kim, S.J. Yoo, H.S. Ahn, W.J. Choi, H.R. Moon, K.M. Lee, M.W. Chun, L.S. Jeong *Bioorg. Med. Chem. Lett.* **2004**, *14*, 2091-2093.

[21] a) L. L. Bennett, Jr., B. J. Bowdon, P. W. Allan and L. M. Rose, *Biochem. Pharmacol.* **1986**, *35*, 4106-4109; b) M. Hasobe, J. G. McKee, D. R. Borcherding, B. T. Keller and R. T. Borchardt, *Mol. Pharmacol.* **1988**, *33*, 713-720.

[22] K. Fukukawa, T. Ueda, T. Hirano, *Chem. Pharm. Bull.*, **1983**, *31*, 1842-1847.

[23] Y.X. Tan, S. Santhanakrishnan, H.Y. Yang, C.L.L. Chai, E.K.W. Tam, *J. Org. Chem*., **2014**, in press. (doi: 10.1021/jo501248e)

[24] S.M. Siddiqi, X. Chen, S.W. Schneller, S. Ikeda, R. Snoeck, G. Andrei, J. Balzarini, E. De Clercq, *J. Med. Chem*., **1994**, *37*, 1382 – 1384.

[25] R. K. Gordon, K. Ginalski, W. R. Rudnicki, L. Rychlewski, M. C. Pankaskie, J. M. Bujnicki and P. K. Chiang *Eur. J. Biochem.* **2003**, *270*, 3507–3517.

[26] L. S. Jeong, S. J. Yoo, K. M. Lee, M. J. Koo, W. J. Choi, H. O. Kim, H. R. Moon, M. Y. Lee, J. G. Park, S. K. Lee, and M. W. Chun *J. Med. Chem.* **2003**, *46*, 201-203.

[27] S. Shuto, T. Obara, M. Toriya, M. Hosoya, R. Snoeck, G. Andrei, J. Balzarini and E. De Clercq, *J. Med. Chem.* **1992**, *35*, 324-331.

[28] R. Snoeck, G. Andrei, J. Neyts, D. Schols, M. Cools, J. Balzarini and E. De Clercq *Antiviral Research,* **1993**, *21*, 197-216.

[29] Y. Kitade, T. Ando, T. Yamaguchi, A. Hori, M. Nakanishia and Y. Ueno *Bioorg. Med. Chem*. **2006**, *14*, 5578–5583.

A number of 3-deazaneplanocin A and neplanocin A analogs were synthesized and tested for their ability to induce synergistic apoptotic activities in cancer cells. Our studies have identified the critical structural features required for biological activities. No discernible direct correlation between these activities and the *S*-Adenosylhomocysteine Hydrolase (SAHH) inhibitory activities was found.

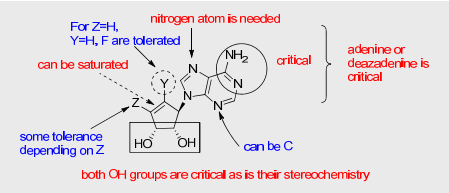

Eric K. W. Tam, Tuan Minh Nguyen, Cheryl Z.H. Lim, Puay Leng Lee, Zhimei Li, Xia Jiang, Sridhar Santhanakrishnan, Tiong Wei Tan, Yi Ling Goh, Sze Yue Wong, Haiyan Yang, Esther H.Q. Ong, Jeffrey Hill, Qiang Yu, and Christina L. L. Chai**

Page No. – Page No.

3-Deazaneplanocin A and Neplanocin A analogs and their effects on apoptotic cell death